BI-OBJECTIVE OPTIMIZATION OF THE PLASMON-ASSISTED LITHOGRAPHY

Design of Plasmonic Nanostructures

Caroline Prodhon[1], Demetrio Macías[2], Farouk Yalaoui[1], Alexandre Vial[2] and Lionel Amodeo[1]
[1]*Laboratoire d'Optimisation des Systèmes Industriels, Institut Charles Delaunay*
[2]*Laboratoire de Nanotechnologie et d'Instrumentation Optique, Institut Charles Delaunay*
Université de Technologie de Troyes, CNRS FRE 2848 - 12, rue Marie Curie, BP-2060 F-10010, Troyes Cedex, France

Keywords: Bi-Objective Optimization, Evolutionary Strategy, Nanolithography.

Abstract: We discuss the influence of the objective function within the context of plasmons-assisted lithography. From previous publications, numerical experiments have shown that the maximization by means of an Evolutionary Strategy of either the visibility or the contrast of the plasmons interference pattern related to the problem does not lead to the ideal situation in which both criteria are maximal. The idea is then to tackle simultaneously these two objective-functions. However, as they are strongly dependent, a more promising strategy is to focus on the minimal and maximal near-field scattered intensities involved in both previously studied criteria. We think that an Evolutionary Strategy based on a bi-objective optimization of these new criteria will provide more satisfactory solutions with respect to the physical constraints imposed.

1 INTRODUCTION

In the few past decades, an important amount of work has been devoted to the application of Evolutionary Strategies (ES) for the solution of different kinds of problems in several scientific disciplines (Djurisic et al., 1997; Hodgson, 2000). The nanotechnologies, a fairly new branch of physics, are not an exception and reported results on the use of these methods is becoming common (Herges et al., 2003; Kildishev et al., 2007). One reason is that ES have proven successful to solve problems on which classical methods fail.

A particular application is for a little studied facet of the inverse physic problem that consists in optimally synthesizing a nanostructure for plasmons-assisted nanolithography. This optimization opens the way to a more intelligent and systematic methodology for the characterization of a nanostructure prior to fabrication. That is, it avoids the waste of time and materials that often results from the iterative adjustment by trial and error of the experimental parameters. Although this approach is commonly employed, there is no guarantee of the optimality of the geometry of the nanosturucture fabricated.

Encouraging results have been obtained thanks to Evolutionary approaches. Nevertheless, the functional form of the objective function and the definition of the search space were not a sufficient condition to obtain a satisfactory physical solution, that in the context of that application required the simultaneous fulfillment of two apparently conflicting objectives. In this paper, we further discuss this issue aiming to have a better understanding on the influence of the definition of the objective function on the solution of a real-world optimization problem in near-field physics.

In Section 2, we formulate the problem and briefly discuss the difficulties for its solution. Section 3 is devoted to the choice of the objective-function and the proposed idea based on bi-objective optimization for the characterization of a nanostructure. We give our main conclusions and final remarks in Section 4.

2 SCATTERING OF LIGHT

We consider the scattering of light from a one-dimensional multilayered geometry (see Fig.1).

The region $x_3 > \frac{d}{2} + \zeta_1(x_1)$ is a homogeneous medium characterized by its refractive index n_0. The region $\frac{d}{2} + \zeta_1(x_1) > x_3 > -\frac{d}{2} + \zeta_2(x_1)$ is filled with a metal with complex frequency-dependent index of

Prodhon C., Macías D., Yalaoui F., Vial A. and Amodeo L. (2009).
BI-OBJECTIVE OPTIMIZATION OF THE PLASMON-ASSISTED LITHOGRAPHY - Design of Plasmonic Nanostructures.
In *Proceedings of the International Joint Conference on Computational Intelligence*, pages 306-309
DOI: 10.5220/0002322403060309

refraction $n_1(\omega)$. The upper and lower interfaces , $\zeta_1(x_1)$ and $\zeta_2(x_1)$, are assumed to be two arbitrarily corrugated surfaces separated by a distance d, which also is the mean thickness of the metallic film. The medium in the region $x_3 < -\frac{d}{2} + \zeta_2(x_1)$ is a homogeneous dielectric of constant refractive index n_2. Although in remainder of the presentation we have considered only three regions for this particular application, this is not a restrictive condition. However, as it will become evident in the following, a larger number of interfaces would unnecesarily increase the complexity of the direct scattering problem, without contributing with additional information to the operational principles of the optimization method employed here.

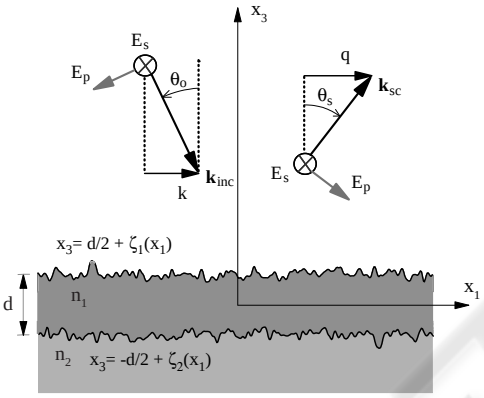

Figure 1: Geometry of the scattering problem.

The plane of incidence is the x_1x_3- plane. With reference to Fig. 1, the surface is illuminated from the region $x_3 > \frac{d}{2} + \zeta_1(x_1)$ with a p- or s- polarized plane wave. The single nonzero component of the electric or magnetic vector of the incident field has the form

$$\psi_2(x_1, x_3|\omega)_{inc} = \psi_o \exp\{i[kx_1 - \alpha_o(k)x_3]\}, \quad (1)$$

where $\alpha_o(k) = \sqrt{(\omega/c)^2 - k^2}$, ω is the frequency of the field, and c is the speed of light in vacuum. A time dependence of the form $\exp(-i\omega t)$ is assumed, but explicit reference to it is suppressed.
As described by (Gu et al., 1993), the application of Green's Integral Theorem to each region in Fig. 1, together with the respective boundary conditions for each interface, lead to the following system of coupled integral equations

$$\begin{aligned}\psi^{(0)}(x_1|\omega)\theta(x_3 - (d/2 + \zeta_1(x_1))) = \psi_{inc}(x_1|w) + \\ + \lim_{\varepsilon\to 0}\int_{-\infty}^{\infty} dx_1' \left[\varphi^{(1)}(x_1'|\omega)H^{(0)}(x_1|x_1')\right] \\ - \lim_{\varepsilon\to 0}\int_{-\infty}^{\infty} dx_1' \left[\chi^{(1)}(x_1'|\omega)L^{(0)}(x_1|x_1')\right], \quad (2)\end{aligned}$$

$$\begin{aligned}0 = \lim_{\varepsilon\to 0}\frac{1}{4\pi}\int_{-\infty}^{\infty} dx_1' \left[\varphi^{(1)}(x_1'|\omega)H^{(11)}(x_1|x_1')\right] \\ - \lim_{\varepsilon\to 0}\frac{1}{4\pi}\int_{-\infty}^{\infty} dx_1' \left[\frac{\varepsilon_1(\omega)}{\varepsilon_0}\chi^{(1)}(x_1'|\omega)L^{(11)}(x_1|x_1')\right] \\ - \lim_{\varepsilon\to 0}\frac{1}{4\pi}\int_{-\infty}^{\infty} dx_1' \left[\varphi^{(2)}(x_1'|\omega)H^{(12)}(x_1|x_1')\right] \\ - \lim_{\varepsilon\to 0}\frac{1}{4\pi}\int_{-\infty}^{\infty} dx_1' \left[\chi^{(2)}(x_1'|\omega)L^{(12)}(x_1|x_1')\right], \quad (3)\end{aligned}$$

$$\begin{aligned}\psi^{(2)}(x_1|\omega) = \\ \lim_{\varepsilon\to 0}\frac{1}{4\pi}\int_{-\infty}^{\infty} dx_1' \left[-\varphi^{(1)}(x_1'|\omega)H^{(21)}(x_1|x_1')\right] \\ - \lim_{\varepsilon\to 0}\frac{1}{4\pi}\int_{-\infty}^{\infty} dx_1' \left[\frac{\varepsilon_1(\omega)}{\varepsilon_0}\chi^{(1)}(x_1'|\omega)L^{(21)}(x_1|x_1')\right] \\ - \lim_{\varepsilon\to 0}\frac{1}{4\pi}\int_{-\infty}^{\infty} dx_1' \left[\varphi^{(2)}(x_1'|\omega)H^{(22)}(x_1|x_1')\right] \\ - \lim_{\varepsilon\to 0}\frac{1}{4\pi}\int_{-\infty}^{\infty} dx_1' \left[\chi^{(2)}(x_1'|\omega)L^{(22)}(x_1|x_1')\right] \quad (4)\end{aligned}$$

and

$$\begin{aligned}0 = \lim_{\varepsilon\to 0}\frac{1}{4\pi}\int_{-\infty}^{\infty} dx_1' \left[\varphi^{(2)}(x_1'|\omega)H^{(s)}(x_1|x_1')\right] \\ - \lim_{\varepsilon\to 0}\frac{1}{4\pi}\int_{-\infty}^{\infty} dx_1' \left[\frac{\varepsilon_2}{\varepsilon_1(\omega)}\chi^{(2)}(x_1'|\omega)L^{(s)}(x_1|x_1')\right], \quad (5)\end{aligned}$$

where $\varepsilon_0 = n_0^2$, $\varepsilon_1(\omega) = n_1^2$ and $\varepsilon_2 = n_2^2$. Also, $\varphi^{(1)}(x_1|\omega)$, $\chi^{(1)}(x_1|\omega)$, $\varphi^{(2)}(x_1|\omega)$ and $\chi^{(2)}(x_1|\omega)$ in Equations (2), (3),(4) and (5), respectively, are known as source functions and are given by

$$\varphi^{(1)}(x_1|\omega) = \psi^{(0)}(x_1, x_3|\omega)\Big|_{x_3 = d/2 + \zeta_1(x_1) + \varepsilon}, \quad (6)$$

$$\chi^{(1)}(x_1|\omega) = \left[-\zeta_1'(x_1)\frac{\partial}{\partial x_1} + \frac{\partial}{\partial x_3}\right]\psi^0(x_1, x_3|\omega)\Big|_{x_3 = d/2 + \zeta_1(x_1) + \varepsilon}, \quad (7)$$

$$\varphi^{(2)}(x_1|\omega) = \psi^2(x_1, x_3|\omega)\Big|_{x_3 = -d/2 + \zeta_2(x_1)}, \quad (8)$$

$$\chi^{(2)}(x_1|\omega) = \left[-\zeta_2'(x_1)\frac{\partial}{\partial x_1} + \frac{\partial}{\partial x_3}\right]\psi^2(x_1, x_3|\omega)\Big|_{x_3 = -d/2 + \zeta_2(x_1)}. \quad (9)$$

The source functions (6) and (7) are the field and its normal derivative evaluated on the interface $d/2 +$

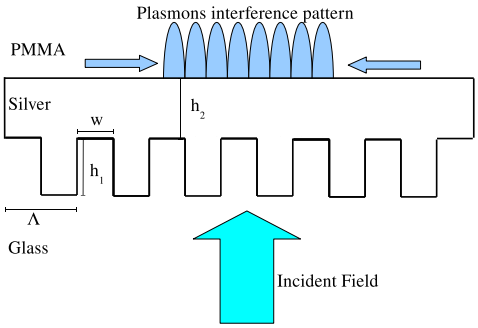

Figure 2: Surface-Plasmons Interference.

$\zeta_1(x_1)$; whereas the source functions (8) and (9) correspond to the field and its normal derivative evaluated on the surface $-d/2+\zeta_2(x_1)$. The kernels of the integral equations (2)-(5) are explicitly written in the appendix A of (Gu et al., 1993).

Following them, the coupled integral equations (2)-(5) are solved numerically to determine the source functions (6)-(9), which are necessary to compute the total field $\psi^{(0)}(x_1|\omega)$ in the region $x_3 > \frac{d}{2}+\zeta_1(x_1)$ or the field $\psi^{(2)}(x_1|\omega)$ transmitted through the metallic film into the region $x_3 < -\frac{d}{2}+\zeta_2(x_1)$.

The total or transmitted intensities can be written as the squared modulus of they respective fields, that is

$$I^{(\alpha)}(x_1|\omega) = |\psi^{(\alpha)}(x_1|\omega)|^2, \qquad (10)$$

where $\alpha = 0,2$

The formalism just described has been extensively used for the solution of different kinds of problems in near- and far-field scattering and SERS (Sanchez-Gil et al., 2002), or in Plasmonics (Giannini and Sanchez-Gil, 2007). A particular application of this fairly new branch of Nanosciences, that has attracted the attention of different research groups, is the Plasmons-Interference-Assisted Nano-Lithography. As shown by (Derouard et al., 2007), this technique offers the possibility to conform the topography of a photosensitive material through the interference of wave-like solutions of Maxwell's Equations called Plasmons. This phenomenon is schematically described in Fig.2, where as a consequence of the interaction bewteen the squared grating and the incident field, two counter-propagating plasmons generate interference pattern on the flat interface of the metallic (silver) film.

In addition to the experimental and numerical evidence presented by (Derouard et al., 2007), some efforts have been conducted to maximize the visibility of the interference pattern depicted in Fig.2, through the optimization of some geometrical features of the nano-structure considered and the illumination conditions. (Macías and Vial, 2008) optimize the visibility

$$V(x_1|p) = \frac{I^{(p)}(x_1|p)_{max} - I^{(p)}(x_1|p)_{min}}{I^{(p)}(x_1|p)_{max} + I^{(p)}(x_1|p)_{min}} \qquad (11)$$

where the components of the vector $p = \{\theta_0, h_1, h_2, w\}^T$ are the variables of interest. The optimization of $V(x_1|p)$ provides feasible solutions with high visibility. However, this approach presents an important drawback as regards a weak contrast

$$C(x_1|p) = I^{(p)}(x_1|p)_{max} - I^{(p)}(x_1|p)_{min} \qquad (12)$$

which implies that there will not be enough power to modify the topography of the photo sensitive material. Based on the fact that

$$V(x_1|p) = \frac{C(x_1|p)}{I^{(p)}(x_1|p)_{max} + I^{(p)}(x_1|p)_{min}}$$

(Prodhon et al., 2009) propose to use C as objective function. This provides better solutions in terms of contrast, while keeping reasonable value of visibility. Furthermore, the objective-variables are closer to the physical feasibility of the context of work. (Prodhon et al., 2009) conclude that the choice of criteria fitness function has significant effects on the results. Nevertheless, the ideal situation in which contrast and visibility are maximal does not seem attainable when these two objective functions are tackled separately.

Another drawback in the formulations of (Macías and Vial, 2008) and (Prodhon et al., 2009) is that their forward scattering solvers are based on the Finite-Difference Time-Domain method (FDTD). Despite its popularity, this approximative numerical method presents important problems of numerical convergence. Also, the accuracy of its results strongly depends on the size of the elementary cell. For this reason, in this work, we propose to use the rigorous numerical integral method described in the previous paragraphs for the computation of $I^{(\alpha)}(x_1|\omega)$.

3 OPTIMIZATION OF THE INTERFERENCE PATTERN

An idea to achieve high quality solutions is to keep a vision the more global as possible on the whole problem, i.e. to carry a search ensuring high values on both C and V. Since C and V are strongly dependent, a bi-objective optimization on these two criteria may not be the best way to obtain the expected results. A more promising strategy is to focus on the near-field scattered intensity involved in both previous studied criteria. Let $I^{(p)}(x_1|p)_{max} = I_{max}$ and

$I^{(p)}(x_1|p)_{min} = I_{min}$, a formulation of C as regard to the maximum and minimum intensity is:

$$Max \quad C(x_1|p) \Leftrightarrow Max \quad (I_{max} - I_{min}) \tag{13}$$

$$\Leftrightarrow Max(I_{max}) \quad and \quad Min(I_{min}) \tag{14}$$

The same transformation can be done on V.

$$Max \quad V(x_1|p) \Leftrightarrow \quad Max \quad (\frac{I_{max} - I_{min}}{I_{max} + I_{min}}) \tag{15}$$

$$\Leftrightarrow \quad Max \quad \frac{(\frac{I_{max}}{I_{min}} - \frac{I_{min}}{I_{min}})}{(\frac{I_{max}}{I_{min}} + \frac{I_{min}}{I_{min}})} \tag{16}$$

Let $\alpha = \frac{I_{max}}{I_{min}}$

$$Max \quad V(x_1|p) \Leftrightarrow \quad Max(\frac{\alpha - 1}{\alpha + 1}) \tag{17}$$

$$\Leftrightarrow \quad Max(\frac{\alpha + 1 - 1}{\alpha + 1} - \frac{1}{\alpha + 1}) \tag{18}$$

$$\Leftrightarrow \quad Max(1 - \frac{2}{\alpha + 1}) \tag{19}$$

$$\Leftrightarrow \quad Max(\alpha) \tag{20}$$

$$\Leftrightarrow \quad Max(I_{max}) \quad and \quad Min(I_{min}) \tag{21}$$

Thus, from (14) and (21):

$$Max \quad V(x_1|p) \Leftrightarrow Max \quad (I_{max}) \quad and \quad Min \quad (I_{min})$$
$$\Leftrightarrow Max \quad C(x_1|p)$$

Even if physical limitations can reduce the expectancy of reaching both $C \approx 1$ and $V \approx 1$, this relation shows that the previous optimization models were weak since a maximization on C should be equivalent to a maximization on V (results not observed until now). Furthermore, it is clear that both I_{max} and I_{min} should be tackled in the process to achieve good results. Thus a bi-objective approach seems more promising. Note though that I_{max} and I_{min} are linked by the electric field scattered in the near-field of the surface. To handle the problem, we propose to apply the Pareto Archived Evolutionary Strategy (PAES). PAES is a multi-objective optimizer which uses a simple local search evolution strategy. It exploits an archive of non-dominated solutions to estimate the quality of new candidate solutions. The validation of this work is under process and should be corroborated by the results from the experiments.

4 CONCLUSIONS

In this paper, we have discussed the influence of the objective function within the context of plasmons-assisted lithography. It has been shown that the maximization by means of an Evolutionary Strategy (ES) of either the visibility or the contrast of the plasmons interference pattern does not lead to the ideal situation in which both criteria are maximal. The idea proposed to obtain more promising results is then to tackle simultaneously two objective functions. However, since the contrast and the visibility are strongly dependent but both involve the near-field scattered intensity, we propose to focus on the maximal and minimal values taken by this function. We suggest the use of an ES based on a bi-objective optimization of these new criteria to provide more satisfactory solutions with respect to the physical constraints imposed.

REFERENCES

Derouard, M., Hazart, J., Lerondel, G., Bachelot, R., and Royer, P.-M. A. P. (2007). Polarization-sensitive printing of surface plasmon interferences. *Opt. Express*, (15):4238–4246.

Djurisic, A., Elazar, J., and Rakic, A. (1997). Modeling the optical constants of solids using genetic algorithms with parameter space size adjustment. *Opt. Comm.*, (134):407–414.

Giannini, V. and Sanchez-Gil, J. A. (2007). Calculations of light scattering from isolated and interacting metallic nanowires of arbitrary cross section by means of green's theorem surface integral equations in parametric form. *J. Opt. Soc. Am. A*, (24):2822–2830.

Gu, Z.-H., Lu, J. Q., and Maradudin, A. A. (1993). Enhanced backscattering from a rough dielectric film on a glass substrate. *J. Opt. Soc. Am. A*, (10):1753–1764.

Herges, T., Schug, A., Merlitz, H., and Wenzel, W. (2003). Stochastic optimization methods for structure prediction of biomolecular nanoscale systems nanotechnology. *Physical Chemistry Chemical Physics*, (14):1161–1167.

Hodgson, R. (2000). Genetic algorithm approach to particle identification by light scattering. *Journal of Colloid and Interface Science*, (229):399–406.

Kildishev, A. V., Chettiar, U. K., Liu, Z., Shalaev, V. M., Kwon, D., Bayraktar, Z., and Werner, D. H. (2007). Stochastic optimization of low-loss optical negative-index metamaterial. *J. Opt. Soc. Am. B*, (24):A34–A39.

Macías, D. and Vial, A. (2008). Optimal design of plasmonic nanostructures for plasmon-interference assisted lithography. *Appl. Phys. B*, (93):159–163.

Prodhon, C., Macias, D., Yalaoui, F., and Amodeo, A. V. L. (2009). Evolutionary optimization for plasmon-assisted lithography. In Springer-Verlag, editor, *Applications of Evolutionary Computing, Evoworkshops*, volume 5484/2009.

Sanchez-Gil, J., Garcia-Ramos, J., and Mendez, E. R. (2002). Electromagnetic mechanism in surface-enhanced raman scattering from gaussian-correlated randomly rough metal substrates. *Opt. Express*, (10):879–886.